

UC Irvine

UC Irvine Previously Published Works

Title

Contact issues in electroluminescent devices from ruthenium complexes

Permalink

<https://escholarship.org/uc/item/4sk149c5>

Journal

Applied Physics Letters, 84(5)

ISSN

0003-6951

Authors

Gorodetsky, Alon A
Parker, Sara
Slinker, Jason D
[et al.](#)

Publication Date

2004-02-02

DOI

10.1063/1.1644918

Peer reviewed

Contact issues in electroluminescent devices from ruthenium complexes

Alon A. Gorodetsky, Sara Parker, Jason D. Slinker, Daniel A. Bernards, Man Hoi Wong, and George G. Malliaras^{a)}

Department of Materials Science and Engineering, Cornell University, Ithaca, New York 14853-1501

Samuel Flores-Torres and Héctor D. Abruña

Department of Chemistry and Chemical Biology, Cornell University, Ithaca, New York 14853-1301

(Received 11 September 2003; accepted 3 December 2003)

We report on the temporal evolution of the current, radiance and efficiency of electroluminescent devices based on films of $[\text{Ru}(\text{bpy})_3]^{2+}(\text{PF}_6^-)_2$ (bpy is 2,2'-bipyridyl) with various electrodes. Under forward bias (with the bottom electrode wired as the anode) the device characteristics were independent of the electrodes used. The situation was different under reverse bias, where differences were observed in the steady-state as well as in the transient characteristics of devices with different electrodes. The origin of this asymmetry is discussed. © 2004 American Institute of Physics.

[DOI: 10.1063/1.1644918]

In recent years, transition metal complexes have received attention as active layers for solid-state electroluminescent devices.^{1–9} The prototypical member of this family is the complex $[\text{Ru}(\text{bpy})_3]^{2+}(\text{PF}_6^-)_2$, where bpy is 2,2'-bipyridyl. In 1999, a group at MIT fabricated devices by simply sandwiching a thin layer of this material between indium–tin oxide (ITO) and Al electrodes and reported luminance exceeding 300 cd/m² at just 3 V.¹ Significant advances have been achieved since then, as questions regarding the ultimate efficiency, response time, color tunability, as well as stability of this class of materials are being addressed.⁹

The mechanism of device operation is similar to the so-called light-emitting electrochemical cells.¹⁰ The PF_6^- counterions are mobile in the film and drift under the influence of applied bias and accumulate near the positively charged electrode.⁹ This accumulation of ionic charge creates a large electric field, which enhances hole injection.¹¹ Holes are injected into the highest occupied molecular orbital (HOMO) of $[\text{Ru}(\text{bpy})_3]^{2+}$, which is a t_{2g} orbital of the metal. At the same time, the depletion of PF_6^- ions near the opposite electrode enhances electron injection. The latter are injected into the lowest unoccupied molecular orbital (LUMO) of $[\text{Ru}(\text{bpy})_3]^{2+}$, which is a π^* orbital of the ligand. The injected electronic carriers migrate towards opposite electrodes and combine to form excited $[\text{Ru}(\text{bpy})_3]^{2+*}$ molecules which phosphoresce, and emit orange–red light.⁹

The performance of organic electroluminescent devices is dominated by the process of charge injection.¹² The latter is strongly dependent on the barrier height at the interface between the electrode and the organic.¹³ As a result, high (low) work function metals are used in organic light-emitting diodes for efficient hole (electron) injection.¹⁴ However, as mentioned above, the redistribution of ionic charge in $[\text{Ru}(\text{bpy})_3]^{2+}(\text{PF}_6^-)_2$ devices enhances the injection of both electrons and holes. In this letter, we investigate the influence of different electrodes on the steady-state as well as the transient characteristics of electroluminescent devices from

$[\text{Ru}(\text{bpy})_3]^{2+}(\text{PF}_6^-)_2$. We find that using different electrodes affects the device characteristics only in reverse bias, where the PF_6^- counterions accumulate near the top (evaporated) electrode. Reasons for this behavior are discussed.

The synthesis of $[\text{Ru}(\text{bpy})_3]^{2+}(\text{PF}_6^-)_2$ as well as the device fabrication and characterization procedures are described elsewhere.⁸ ITO as well as ITO coated with a 5 Å Pt layer were used as bottom electrodes. Pt was deposited on top of the ITO through a shadow mask at a rate of 1 Å/s using e-beam deposition. In addition to all cleaning steps described in Ref. 8, the substrates received a final UV/ozone treatment just before being moved into a nitrogen glove box for deposition of the $[\text{Ru}(\text{bpy})_3]^{2+}(\text{PF}_6^-)_2$ films. The top electrodes consisted of 200 Å thick Au, Ag, or Al films deposited via thermal evaporation at a rate of 1–5 Å/s. The top electrode deposition and the subsequent device characterization took place inside a nitrogen glove box to avoid exposure of the samples to ambient.

The radiance was corrected for the difference in transmittance of the Pt coated ITO electrode. This was done by dividing the radiance from such a device by 0.93, which is the transmittance of the Pt layer. The latter was measured at 633 nm, which is close to the emission peak $\lambda_{\text{max}}=609$ nm of $[\text{Ru}(\text{bpy})_3]^{2+}(\text{PF}_6^-)_2$,⁸ using a He–Ne laser beam at normal incidence. A similar correction was employed for the various top electrodes, where the influence of different reflectances was removed. This was done by assuming that photons are emitted with equal probability in the forward direction (where they exit through the ITO), and in the backward direction (where they get reflected by the top electrodes and exit through the ITO). The reflectance of the various top electrodes (0.83 for Ag, 0.69 for Al and 0.41 for Au) was measured at normal incidence, at 633 nm, and the radiance was scaled to that from a hypothetical device with a 100% reflecting top electrode. These corrections were necessary in order to allow a quantitative comparison among devices with different electrodes. As a result, the values presented in Figs. 1 and 2 are not the true external quantum efficiencies, since they have been normalized according to the above procedure.

Two device runs are discussed in this letter. In the first

^{a)}Author to whom correspondence should be addressed; electronic mail: george@ccmr.cornell.edu

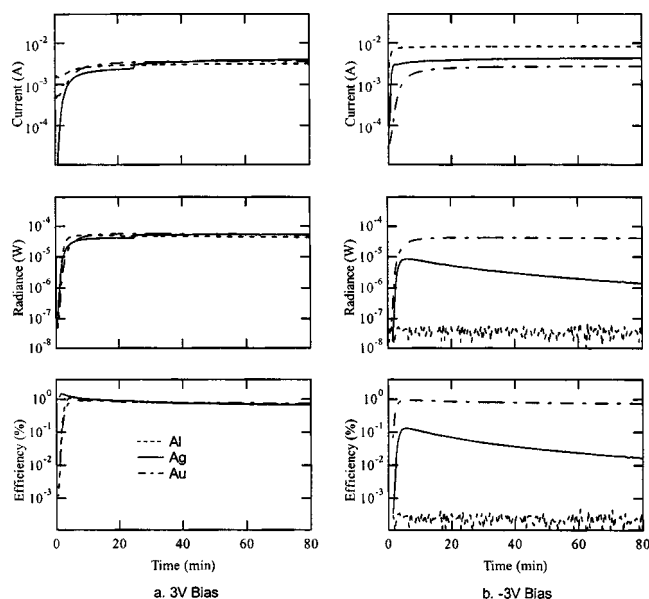


FIG. 1. Temporal evolution of the current, radiance and efficiency of ITO/[Ru(bpy)₃]²⁺(PF₆⁻)₂/M devices under forward (a) and reverse (b) bias. M stands for Al, Ag, or Au. The radiance and efficiency under reverse bias for the device with the Al top electrode was below the noise floor of our detector.

one, all devices had an ITO bottom electrode and different top electrodes. The temporal evolution of the current, radiance and efficiency of these devices is shown in Fig. 1. In the second run, the devices had Au top electrodes, and ITO or Pt coated ITO as bottom electrodes. The data from these devices are shown in Fig. 2. The thickness of the [Ru(bpy)₃]²⁺(PF₆⁻)₂ films in the first and second device runs was 105 ± 5 and 90 ± 5 nm, respectively.

We first discuss the data under forward bias, where the bottom electrode (ITO or Pt covered ITO) is biased positive with respect to the top one. The relevant data are shown in Figs. 1(a) and 2(a). In this configuration, the PF₆⁻ counterions accumulate near the bottom electrode, which injects

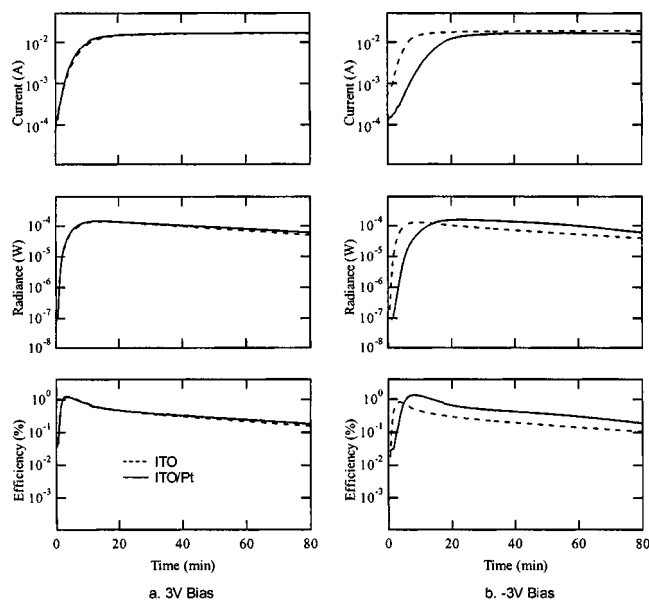


FIG. 2. Temporal evolution of the current, radiance and efficiency of M/[Ru(bpy)₃]²⁺(PF₆⁻)₂/Au devices under forward (a) and reverse (b) bias. M stands for ITO or Pt coated ITO.

holes, while electrons are injected from the top electrode. Overall, the data are virtually identical within each device run, which signifies that hole (electron) injection is not affected by the choice of bottom (top) electrode. The fact that charge injection is independent of the electrode used indicates that the barrier lowering induced by the ionic space charge is significantly strong to make the contacts ohmic regardless of the electrode work function.¹¹ Therefore, electron and hole currents are balanced in this bias configuration and the devices operate at their maximum efficiency, which is determined by the photoluminescence yield of the [Ru(bpy)₃]²⁺(PF₆⁻)₂ film.¹²

More specifically, as seen in Fig. 1(a), Au, Ag, and Al top electrodes (with work functions of 5.1, 4.26, and 4.28 eV, respectively¹⁵) inject electrons with the same efficiency. As a result, there is no need to use low work function metals, which are the Achilles heel of organic light-emitting diodes.¹⁴ The two bottom electrodes (ITO and Pt covered ITO) also inject holes with the same efficiency, as seen in Fig. 2(a). Coating ITO with ultrathin Pt films is known to increase the former's work function.¹⁶ In particular, Pt coated ITO films prepared earlier in an identical way to that described here were found to have a 0.6 eV higher work function than plain ITO.¹⁷ However, as evident in Fig. 2(a), this change in work function of the bottom electrode does not result in any enhancement in hole injection. Therefore, there is no need to use electrodes with a work function higher than that of ITO for efficient hole injection in [Ru(bpy)₃]²⁺(PF₆⁻)₂ devices.

The situation is markedly different under reverse bias [Figs. 1(b) and 2(b)]. In this configuration, the PF₆⁻ counterions accumulate near the top electrode, which injects holes, while electrons are injected from the bottom electrode. In Fig. 1(b), the current is shown to depend on the top electrode, changing in order $I(\text{Al}) > I(\text{Ag}) > I(\text{Au})$. This indicates that hole injection depends on the metal, in contrast with what was observed under forward bias [Fig. 2(a)]. The scaling of the currents is the opposite of what one would anticipate based on work function values. Au has the highest work function, but injects holes least efficiently. Possible causes of such behavior are discussed in more detail below. The fact that changing the hole-injecting electrode leads to a change in total device current indicates that the devices in Fig. 1(b) are not current balanced; rather, the current is dominated by holes.¹²

An even larger variation is observed in the radiance of the devices, shown in Fig. 1(b). The device with the Al top electrode does not show any emission under reverse bias. This is in agreement with earlier observations by Rudman and Rubner.⁵ In addition, a visible change of the Al electrode was obvious to the naked eye after 90 min at reverse bias. The mechanism probably involves electrochemically induced oxidation of the Al (which is promoted in this bias configuration) followed by hydrolysis of [Ru(bpy)₃]²⁺ to form [Ru(bpy)₂(H₂O)₂]²⁺. The latter compound has been identified as a quencher in [Ru(bpy)₃]²⁺ based devices.¹⁸ The radiance of the device with the Ag electrode is lower than that of the device with the Au electrode, and decays faster too. This indicates that Ag electrodes are also susceptible to a similar degradation mechanism, although at a diminished

rate compared to Al. Au, on the other hand, appears to be stable in the time scale of the experiment.

Abkowitz *et al.*¹³ recently studied the influence of metal deposition on the characteristics of devices based on organic semiconductors. Measurements of injection efficiency revealed that top electrodes are usually inferior injectors compared to bottom ones. Namely, when an organic semiconductor was sandwiched between two Au electrodes, the bottom Au contact (which was formed by solution casting the organic on top of a Au electrode) was ohmic, while the top one (which was formed by evaporation of Au on the organic) was found to be current limiting. The inferior injection from the top contact was attributed to deposition-induced damage of the organic film just below the surface of the top electrode.¹³ The exact nature of the damage remains elusive.¹³ Ioannidis *et al.*¹⁹ studied this effect further and found top Au contacts evolve over time and eventually “heal,” i.e., reach the same injection efficiency as bottom ones.

A similar mechanism, where deposition-induced damage takes place at the $[\text{Ru}(\text{bpy})_3]^{2+}(\text{PF}_6^-)_2$ /top electrode interface, can explain the observed differences between forward and reverse bias data. Damage at the interface might be related to effects such as decomposition of the $[\text{Ru}(\text{bpy})_3]^{2+}$ molecules, crystallization of the $[\text{Ru}(\text{bpy})_3]^{2+}(\text{PF}_6^-)_2$ film below the electrode surface, and diffusion of metal into the $[\text{Ru}(\text{bpy})_3]^{2+}(\text{PF}_6^-)_2$ film. These effects, in turn, can inhibit efficient packing of PF_6^- counterions near the top electrode, and lead to incomplete cancellation of the barrier for hole injection. This would result in hole current that is less than that injected from an ohmic contact, and it seems to be the case for the Au top electrode. As shown in Figs. 1(a) and 1(b), the current flowing in the ITO/ $[\text{Ru}(\text{bpy})_3]^{2+}(\text{PF}_6^-)_2$ /Au device is higher under forward than it is under reverse bias. The rectification, however, was found to disappear at 6 V,⁸ where a larger buildup of ionic space charge makes all contacts ohmic. In addition, the rectification at 3 V was found to disappear a few days after device preparation, in agreement with the work of Ioannidis *et al.*¹⁹

An additional mechanism might be in action for the Al (and, to a lesser extent, for the Ag) top electrode, where electrochemical oxidation of the metal could lead to an increase in the current drawn from the device. This is supported by the fact that the reverse bias current in the ITO/ $[\text{Ru}(\text{bpy})_3]^{2+}(\text{PF}_6^-)_2$ /Al device is higher than the forward bias current [Figs. 1(a) and 1(b)]. Work is ongoing to pinpoint the exact nature of $[\text{Ru}(\text{bpy})_3]^{2+}(\text{PF}_6^-)_2$ /top electrode interfaces.

It turns out that whatever damage takes place near the top contact also influences charge injection from the bottom contact. This is seen in Fig. 2(b), where the transient response of devices with different bottom electrodes is markedly different. Namely, ITO is shown to inject electrons more efficiently than Pt coated ITO *at shorter times*. This is consistent with the fact that ITO has a lower work function than Pt coated ITO,¹⁷ resulting in a lower initial barrier for elec-

tron injection. As a result, fewer uncompensated $[\text{Ru}(\text{bpy})_3]^{2+}$ ions are needed near the ITO contact to make it ohmic. Over time, however, both devices reach the same current and also show the same maximum radiance and efficiency. This indicates that, at steady state, the density of uncompensated $[\text{Ru}(\text{bpy})_3]^{2+}$ ions near the bottom contact is the same. Coating the ITO with Au instead of Pt resulted in the same trend (not shown here).

In conclusion, we have fabricated electroluminescent devices based on films of $[\text{Ru}(\text{bpy})_3]^{2+}(\text{PF}_6^-)_2$ with different top and bottom electrodes. Under forward bias, where the PF_6^- counterions accumulate near the bottom electrode, the device behavior was independent of the electrodes used. This indicated that the devices operated at their optimal point. The situation was quite different under reverse bias, where the PF_6^- counterions accumulate near the top electrode. Different top electrodes were found to inject holes with different efficiency. The same was true for bottom electrodes, however, only at earlier times. The differences between forward and reverse bias are consistent with damage induced in the $[\text{Ru}(\text{bpy})_3]^{2+}(\text{PF}_6^-)_2$ /top electrode interface during metal deposition.

This work was supported by the National Science Foundation (Career Award No. DMR-0094047) and by the Cornell Center for Materials Research (CCMR), a Materials Research Science and Engineering Center of the National Science Foundation (Grant No. DMR-9632275).

- ¹E. S. Handy, A. J. Pal, and M. F. Rubner, *J. Am. Chem. Soc.* **121**, 3525 (1999).
- ²F. G. Gao and A. J. Bard, *J. Am. Chem. Soc.* **122**, 7426 (2000).
- ³H. Rudmann and M. F. Rubner, *J. Appl. Phys.* **90**, 4338 (2001).
- ⁴S. Bernhard, X. Gao, G. G. Malliaras, and H. D. Abruña, *Adv. Mater. (Weinheim, Ger.)* **14**, 433 (2002).
- ⁵C. Y. Liu and A. J. Bard, *J. Am. Chem. Soc.* **124**, 4190 (2002).
- ⁶H. Rudmann, S. Shimada, and M. F. Rubner, *J. Am. Chem. Soc.* **124**, 4918 (2002).
- ⁷M. Buda, G. Kalyuzhny, and A. J. Bard, *J. Am. Chem. Soc.* **124**, 6090 (2002).
- ⁸S. Bernhard, J. A. Barron, P. L. Houston, H. D. Abruña, J. L. Ruglovsky, X. Gao, and G. G. Malliaras, *J. Am. Chem. Soc.* **124**, 13624 (2002).
- ⁹J. Slinker, D. Bernards, P. L. Houston, H. D. Abruña, S. Bernhard, and G. G. Malliaras, *Chem. Commun.* **19**, 2392 (2003).
- ¹⁰Q. B. Pei, G. Yu, C. Zhang, and A. J. Heeger, *Science* **269**, 1086 (1995).
- ¹¹J. C. de Mello, N. Tessler, S. C. Graham, and R. H. Friend, *Phys. Rev. B* **57**, 12951 (1998).
- ¹²G. G. Malliaras and J. C. Scott, *J. Appl. Phys.* **83**, 5399 (1998).
- ¹³M. Abkowitz, J. S. Facci, and J. Rehm, *J. Appl. Phys.* **83**, 2670 (1998).
- ¹⁴J. C. Scott and G. G. Malliaras, in *Conjugated Polymers*, edited by G. Hadziioannou and P. F. van Hutten (Wiley-VCH, New York, 1999), Chap. 13.
- ¹⁵D. R. Lide, *CRC Handbook of Chemistry and Physics*, 84th ed. (Chemical Rubber, New York, 2003).
- ¹⁶S. M. Tadayyon, K. Griffiths, P. R. Norton, C. Tripp, and Z. Popovic, *J. Vac. Sci. Technol. A* **17**, 1773 (1999).
- ¹⁷Y. Shen, D. B. Jacobs, G. G. Malliaras, G. Koley, M. G. Spencer, and A. Ioannidis, *Adv. Mater. (Weinheim, Ger.)* **13**, 1234 (2001).
- ¹⁸G. Kalyuzhny, M. Buda, J. McNeill, P. Barbara, and A. J. Bard, *J. Am. Chem. Soc.* **125**, 6272 (2003).
- ¹⁹A. Ioannidis, J. S. Facci, and M. A. Abkowitz, *J. Appl. Phys.* **84**, 1439 (1998).